(8) Adhesion and Aggregation Mechanisms of Methanogenic Sludge Consortia Developed in an UASB Reactor

ＵＡＳＢ反応器における嫌気性細菌群の付着・集塊機構の解明

I-Cheng Tseng*, Hideki HARADA*, Sy-Ying Chen Wang**, Kiyoshi MOMONOI*
曽怡禎、原田秀樹、陳是瑩、桃井清至

ABSTRACT: In order to clarify the key-mechanisms of self-immobilization of anaerobic sludge consortia, biofilms at various growth stage were obtained over 120 days by installing slide-glass plates as a substratum in an UASB (upflow anaerobic sludge blanket) reactor. Biofilms taken out from the reactor at appropriate time intervals were forwarded to morphological observation with SEM and fluorescence microscopy, extracellular biopolymer analysis and the viable cell counting. The progression of biofilm could be differentiated into four sequent stages: adhesion (until 7 days), clump (8—28 days), conglomerate (29—80 days), and aggregate stage (81—120 days). A strong analogy in self-immobilization of anaerobic microorganisms was observed between biofilm formation and granulation. Entanglement of *Methanothrix* filaments served to provide other bacterial groups with sites for colonization and to conjoin adjacent microcolonies with each other to form a further extended aggregate. *Methanobrevibacter* spp. and *Methanothrix* spp. showed superior capability in adhering to substratum. The population sizes of hydrogenotrophic and acetotrophic methanogens were of the same order of magnitude, i.e. 1.4—1.6 × 10^9/g· biomass at the final of the aggregate stage.

Keywords: Adhesion, Aggregation, Anaerobic treatment, Biofilm formation, Granulation, UASB reactor.

INTRODUCTION

Anaerobic technology has been successfully developed for treatment of certain kinds of industrial wastewaters in the last decade. This technology comprehends mainly fixed bed, fluidized bed and UASB (upflow anaerobic sludge blanket) reactors. All these types of anaerobic reactors employ in common the concept of self-aggregation of anaerobic microorganisms for enhancement of biomass retainment [1,2].
Anaerobic fixed bed reactor and fluidized bed reactor perform this function by means of biofilm formation onto stationary carriers and onto moving carriers, respectively. UASB reactor fulfills the task of high biomass retainment by means of granulation. Hence, granulation can be regarded as a manifestation of spherical biofilm without "explicitly-provided" carriers. In case of UASB reactor small inert particulates contained a priori in a seed source or precipitates formed in the reactor serve as nuclei for initial adhesion of microorganisms[3,4]. Therefore, it can be said that both biofilm formation and sludge granulation commonly involve bacterial adhesion process and succeeding aggregation process.
So far considerable concerns have been focused, but independently, on mechanism of either biofilm formation or granulation. However, there must be a definite analogy in mechanisms between biofilm formation and granulation. It is of great use to find out key mechanisms of self-immobilization of anaerobic microorganisms for betterment of anaerobic advanced wastewater technology.

*Department of Civil Engineering, Nagaoka University of Technology.
**Department of Biology, National Cheng Kung University, Taiwan.

On this background, we intended in this study to clarify the ubiquitous mechanism of self-immobilization by means of simultaneous observation of biofilm formation and granulation taking place in an identical reactor. For this purpose the morphology of biofilms at various growth stages was compared with that of granulted sludge, both developed in the identical UASB reactor. In addition, behaviors of extracelluar polymer and the viable cell number of biofilm were examined in the course of biofilm development.

MATERIALS AND METHODS

Apparatus and sampling

A semi pilot-scale UASB reactor that had been operated over 6 years in our laboratory was used to provide a site for anaerobic biofilm formation. The UASB reactor consisted of a column with 20 cm in inner diameter and 3 m in height and a GSS (Gas-solids separator) portion, as shown in Fig. 1-A. The total volume of the reactor was 175 *l* (column portion: 94 *l*, GSS portion: 81*l*). The reactor has been maintained in a steady state for more than one year by continuously feeding a solution made up of commerical milk and inorganic supplements. Reactor operation conditions were as followers: Influent strength, 3,800 mg COD/*l*; Volumetric loading rate, 6 kg COD/m^3· d; COD removal, 90-92%; HRT, 0.6 days.

Slide-glass plates (each: 75 × 24 mm) and cover-glass plate (18 × 24 mm) were used as biofilm attached-growth substrata. Five slide-glass plates and five cover-glass plates were installed to each supporting device, as shown in Fig. 1-B. A total of 22 sets of supporting device was placed in the sludge blanket portion of the UASB column by hanging from GSS portion (Fig. 1-A). Accordingly slide-glass and cover-glass plates installed in the reactor totaled 110 each.

Biofilms taken out from the reactor were immersed in a sterile saline solution at pH 7.0 (0.85% NaCl) for 1 minute quiescently. The sterile saline solution was purged with N_2 for 20 min before using. The cells remaining on the slide were considered to be attached and compulsorily removed by ultrasonication (Sonifer, Branson Co.) at 35 W for 90 s under N_2 atmosphere in an ice bath. Samples of slide-glass plates were used for biomass determination, extracellular polymer (ECP) analysis and enumeration, and those of cover-glass plates were used for microscopic observation. Biomass and ECP were determined in triplicate using three slide-glass plates each.

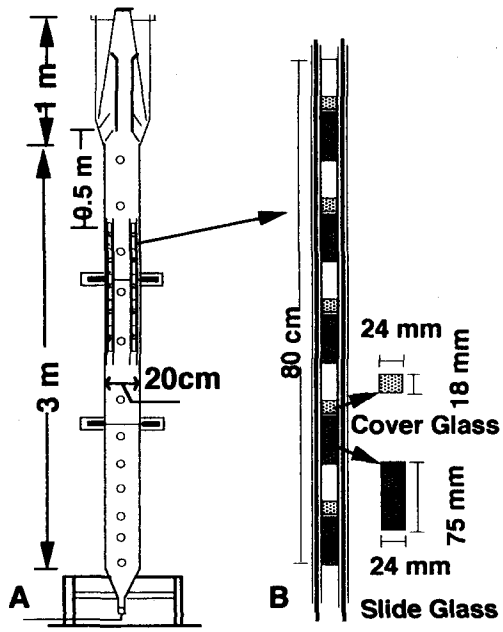

Fig. 1 Experiment set-up.
A: UASB reactor in which the devices shown in Fig. 1-B were installed.
B: Supporting device for placement of slide-glass and cover-glass plates as attachment substrata.

Enumeration

The most-probable number (MPN) method (n=3) was used for enumeration of methanogenic bacteria (MPB) and propionate degrading acetogen (PDA). MPN tests were done in Bellco glass tubes (Bellco Inc. England) containing 9 ml of growth medium with 20 mM substrate and a gas phase of N_2-CO_2 (70:30%, v/v). For enumeration of hydrogenotrophic methanogen (H-MPB), H_2-CO_2 (80:20%, v/v) was filled in 6 ml gas phase as a substrate.

The ingredients of the medium (g/l) were as follows: KH_2PO_4, 0.2; NH_4Cl, 1.0; $MgCl_2.6H_2O$, 0.1; NaCl, 0.3 $NaHCO_3$, 1.0; Yeast extract, 0.2; Cysteine HCl, 0.25; $Na_2S.9H_2O$, 0.25; Resazurine, 0.0002; and 10 ml of Zeikus[5] trace mineral solution. Sodium sulfide was added separately after autoclaving and then the pH of the medium was adjusted to 7.0-7.2 with 0.1 N HCl. After 3 months of incubation at 35°C, methane content was checked by gas chromatography. There are two alternative procedures for enumeration of PDA: one with inoculation of hydrogenotrophic bacteria in the respective test-tubes in advance, and the other without the inoculation. We employed the latter method, since MPN results would be significantly dependent on the type (species and strain) of the hydrogen scavenging partner, and the cell number of H-MPB is, in general, far higher than that of PDA.

Agar-shake method was employed in this study for enumeration of sulfate reducing bacteria (SRB). The screw-capped glass tubes (15 mm × 18 cm) with butyl-rubber stopper and a gas phase of N_2-CO_2 (70:30%) were used. Acetate (20 mM), propionate (20 mM) and lactate (25 mM) were used as a respective electron donor for sulfate reducing bacteria enumeration. The electron donors above-mentioned were added to medium G of Postgate[6] with 0.01% thioglycollate and 0.01% ascorbateas as reducing reagents. In addition, the medium contained 0.02% of yeast extract, 0.01% of Fe_2SO_4 and 0.002% of resazurine. The reducing agents and Fe_2SO_4 were supplemented separately after autoclaving the medium. The pH of the medium was adjusted to 7.0-7.2 with 1 N HCl. Three tubes each dilution was used for enumeration of sulfate reducing bacteria. Incubation was made for 30 days at 35 °C.

Extracellular polymer analysis

ECP was obtained by hot-water extraction method[7]. Samples were heated in an autoclave at 90 °C for 10 min and then centrifuging at 15,000 rpm for 15 min at 4 °C, followed by filtration through 0.22 μm membrane. Carbohydrate content of ECP was measured by phenol-sulfuric acid method of Dubois *et al.*[8] using glucose as a standard. Protein content was determined by Lowery method[9] and bovine serum albumen was used as a standard. Alcian-blue staining was used for observation of polysaccharide of ECP.

Microscopic examination

Fresh samples were observed by optical and fluorescent microscopy and some of samples were also stained with crystal violet prior to observation. For scanning electron microscopy (SEM), samples were washed with 0.85% NaCl solution and then fixed with 4% glutaraldehyde in 0.1M cacodylate buffer (pH 7.2) for 3 hr at 4 °C, followed by washing three times with cacodylate buffer. Dehydration was made in a graded ethanol series of 10%, 25%,. 50%, 75% and 90% for 15 min for each step. The samples were then dehydrated in 95% ethanol for 20 min two times and finally in 100% for 30 min three times. After dehydration the samples were treated with iso-amylacetayte for 1—2 hr and then by critical-point drying. After all the dehydration steps, the samples were glued onto stub and coated with gold for SEM examination.

RESULTS

Morphological observation of biofilm development

Routine SEM observation of biofilm development was made over 120 days using samples taken from UASB reactors at appropriate time intervals. Fig.2 shows representative examples at different time stages. SEM and optical microscopic (both under phase contrast and florescence) observations revealed the overall progression of biofilm formation on glass substrata could be differentiated into four sequent stages according to the distinction in morphological change: adhesion (upto the day 7: Fig.2A), clump (day 8—28: Fig.2B), conglomerate (day 29—80: Fig.2C) and aggregate stages (day 81—120: Fig.2D).

The first stage corresponded to the duration in which initial adhesion of suspended microorganisms occurred. The second stage is characterized by formation of clump structures (microcolonies). During the third stage the individual clump structures became spread, and connected with each other, covering the whole substrata surface. And finally biofilms became matured and reached equilibra in the fourth stage.

Adhesion stage: The onset of adhesion of two morphological types of methanogen occurred instantaneously within the first day. One was rod with tapered ends, having strong green-yellow florescence under epifluoresence microscopy, which resembled *Methanobrevibacter* spp. and the other was bamboo-shaped rod with flat-end septum similar to *Methanothrix* spp.. *Methanothrix* formed readily long chained filaments in the adhesion stage. Attachment of *Methanobrevibacter*-like organisms was performed by fimbriae appendages, as shown in Fig.3-A, whereas no appendage structure was observed in attachment of *Methanothrix* . No emergence of *Methanosarcina* spp. occurred during the adhesion stage.

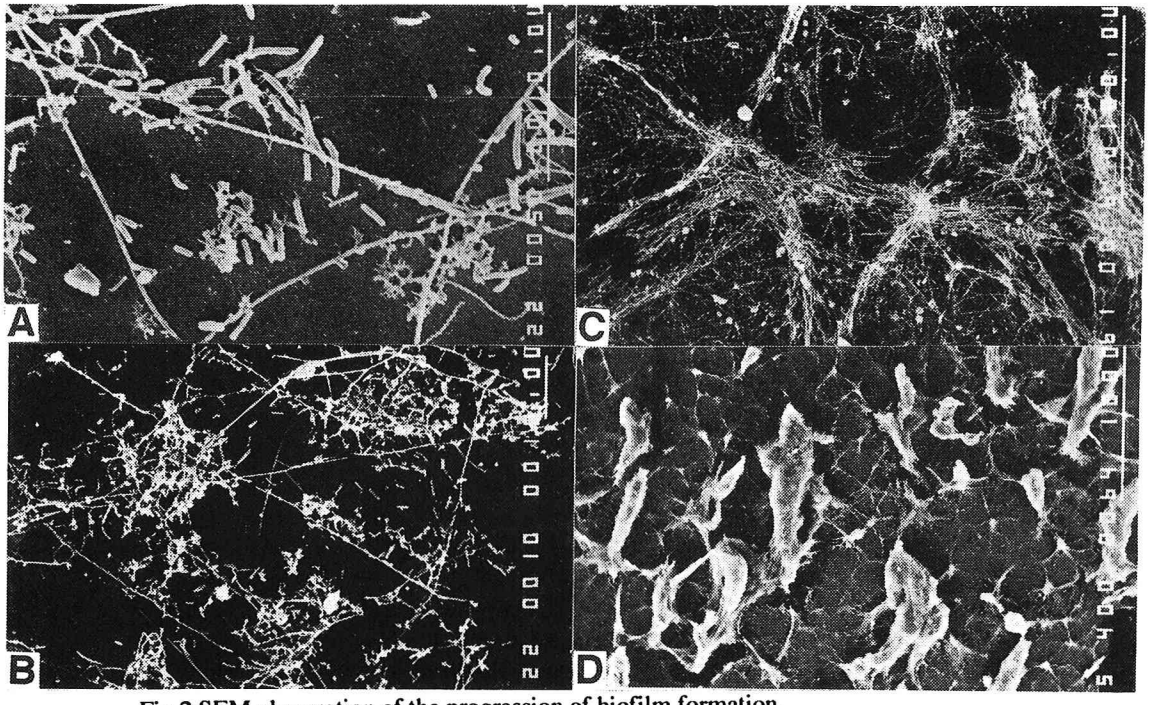

Fig.2 SEM observation of the progression of biofilm formation.
A: The adhesion stage (the day 7). Bar: 10 μm.
B: The clump stage (the day 14). Bar: 10 μm.
C: The conglomerate stage (the day 56). Bar: 100 μm.
D: The aggregate stage (the day 120). Bar: 1000 μm.

Clump stage: The initiation of the second stage was featured by the emergence of microclonies (clumps) with a size of 10-20 μm formed on crossing-points of interwining *Methanothrix*-like filaments (Fig.3B). The clump structure was heterogeneous, containing a diversity of cell morphology including *Methanobrevibacter*-like organisms. Dense extracellular polymers, which reacted positively with Alcian-blue stain, were also found in the clumps. In the late of this stage the presence of coccoid bacteria in the clumps became significant, which possessed high intensity of green fluorescence and were presumably *Methanosarcinamazei*. The color of central portions became black as clump regions stretched out.

Conglomerate Stage: The microcolonies that had come to appearance in the preceding stage proceeded to develop their size during the conglomerate stage. Elongation of *Methanothrix* filaments in all directions incorporated adjacent microcolonies into a larger conglomerate (Fig. 2-C). High magnification SEM observation revealed that web-like structure of entangling *Methanothrix* filaments entrapped various types of organisms and inert ingredients inside (Fig. 3-C).

Aggregate Stage: During the aggregate stage continuing stretch-out of *Methanothrix* filaments came to form larger aggregates with a size of 30-150 μm, by combining adjacent conglomerate, covering thickly the whole substratum surface (Fig. 2-D). Each aggregate was thoroughly surfaced with entanglement of *Methanothrix* filaments. Fig.4-A shows the optical micrograph of the aggregate structure under bright field observation. The same field revealed strong green-yellow fluorescence under epifluorescence illumination (Fig.4-B). The biofilm thickness attained finally about 8 mm on average at the aggregate stage, as shown in Fig. 5.

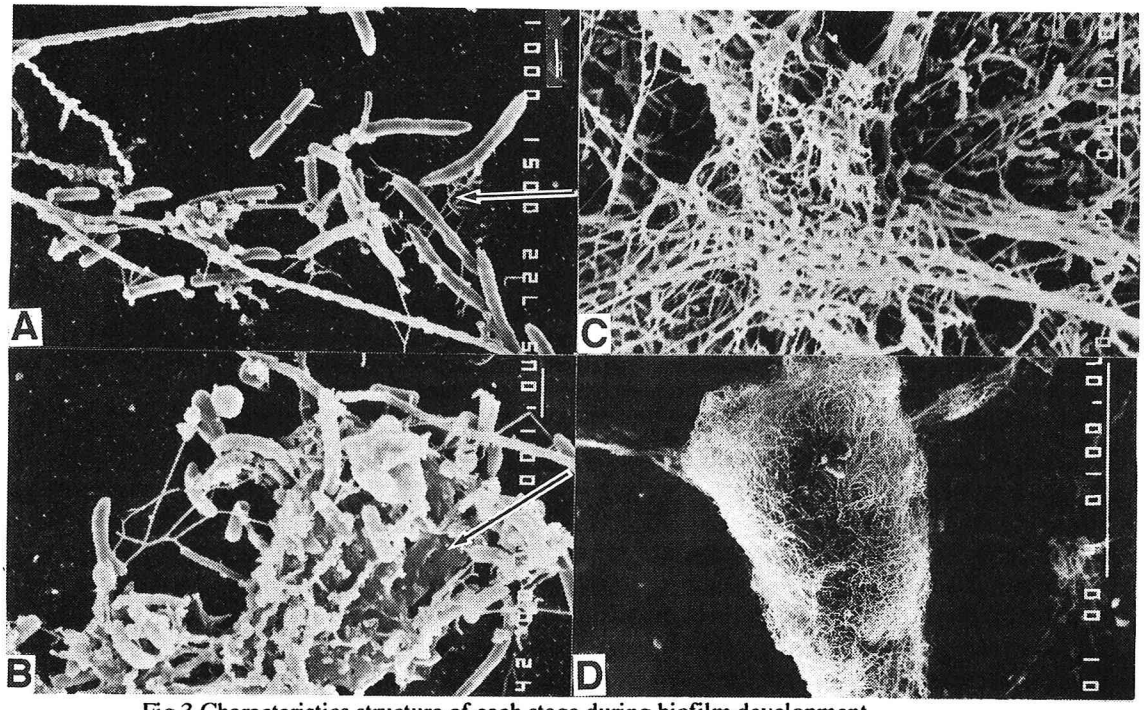

Fig.3 Characteristics structure of each stage during biofilm development.
A: Adhesion of *Methanobrevibacter*-like organism with fimbriae appendages indicated by arrow during the adhesion stage. Bar: 1.0 μm.
B: Structure of microcolony containing a diversity of cell types and polymer material indicated by arrow during the clump stage. Bar indicates 1.0 μm.
C: Enlarged colonization entrapping a diversity of cell morphology and inorganic precipitates during the conglomerate stage. Bar: 10 μm.
D: Formation of aggregate covered with intertwining *Methanothrix* filaments during the final stage. Bar: 100 μm.

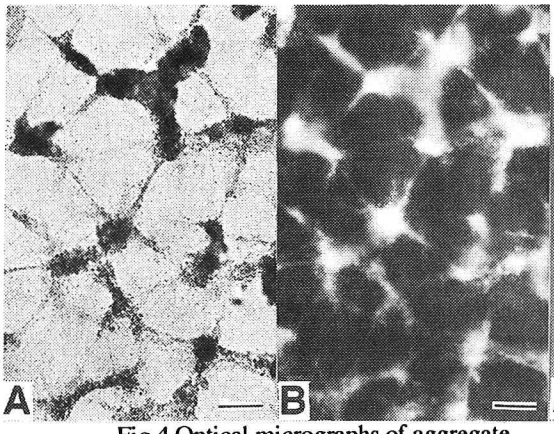

Fig.4 Optical micrographs of aggregate structure developed on 90 th day.
A: Under bright field. Bar: 100 μm.
B: Under epifluoresence illumination of the identical field.

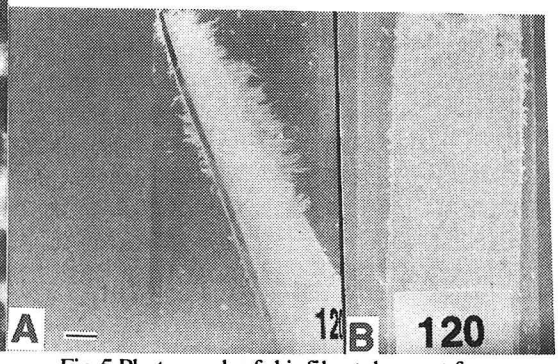

Fig.5 Photograph of biofilm taken out from the reactor on 120th day.
A: Side view. Bar: 5 mm. B: Front view.

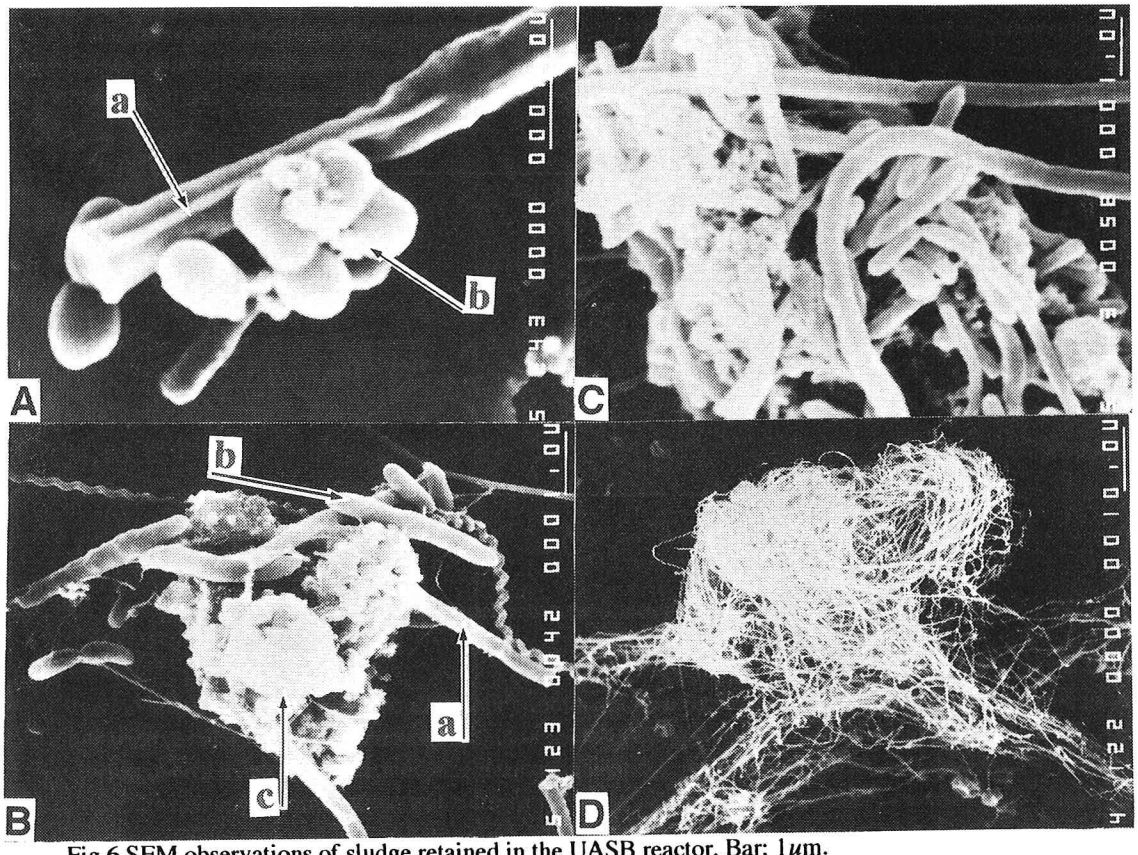

Fig.6 SEM observations of sludge retained in the UASB reactor. Bar: 1μm.
A. Attachment of *Methanosarcina*-like organism (arrow a) onto *Methanothrix*-like organism (arrow b).
B. Formation of microcolony containing *Methanothrix*-like (arrow a), *Methanobrevibacter*-like (arrow b) and *Methanosarcina*-like organisms (arrow c). Bar: 1μm.
C. Enlargement of microcolony and elongation of *Methanothrix*-like filament. Bar: 1μm.
D. Formation of aggregate by interweaving *Methanothrix*-like filament. Bar: 10 μm.

Morphological observation of sludge retained in UASB

Granular sludge consortia taken out from the top of sludge bed portion of the UASB reactor was also examined by SEM and optical microscope, in order to find out analogous mechanism in self-immobilization between biofilm formation and granulation (Fig. 6-A through 6-D).

Fig.6-A clearly shows that *Methanothrix*-like organism provided a site for attachment of other bacteria including *Methanosarcina*-like organism, in granulation process too. Fig. 6-B presents the formation of microcolony similar to that observed in the clump stage of biofilm development (Fig. 3-B). Various types of bacteria were deposited onto the microcolony, involving *Methanothrix*-like, *Methanobrevibacter*-like and *Methanosarcina* like organisms. Fig. 6-C indicates that elongation of *Methanothrix* filaments donated appropriate microhabitats to diversified cell types, which were embedded by function of polymer material as a cementing medium. This structure seems to be a consequence of enlargement of microcolony given in Fig. 6-B. Fig. 6-D shows the intertexture structure of an aggregate formed by interweaving filaments of *Methanothrix* that is analogous to that given in Fig. 3-D.

Variation in biomass and ECP contents

Fig.7 shows the time course of biofilm development, expressed as the amount of biofilm attached (dry weight) per unit glass area. The attached biomass increased steadily up to 3.30 mg/cm^2 throughout the whole period. Although the change in attached biomass was not substantial during the first (adhesion) and the second (clump) stages, it exhibited an exponential growth mode during the conglomerate stage. Followingly biomass development became saturated in the aggregate stage, reaching an equilibrium value around 3.25-3.30 mg/cm^2, at which biofilm thickness attained 8 mm on average.

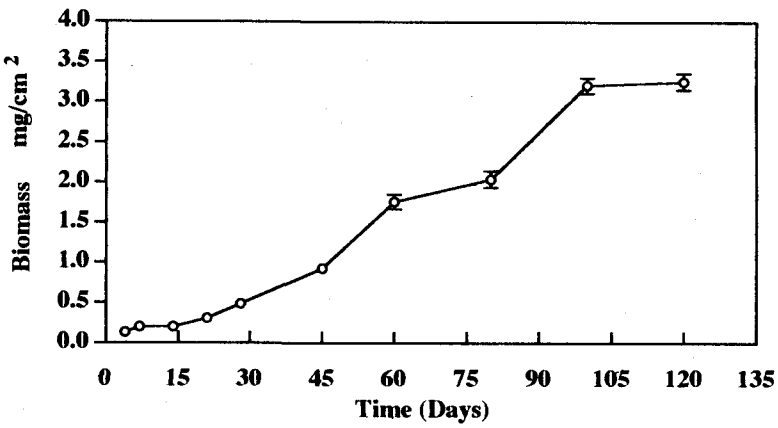

Fig. 7 Time course of biomass per substratum area.

Fig.8 shows the time-variation in carbohydrate and protein contents of extracted ECP over 120 days, expressed as per unit substratum area and as per unit weight of biomass. The contents of carbohydrate and protein based on substratum area increased consistently with time elapsed, i.e. in association with biomass increment. In contrast, those contents on the basis of biofilm weight exhibited different behaviors each other. The carbohydrate content increased up to 21.4 μg/mg· biomass at the middle of the clump stage, and afterward began to decline. It reached finally in the aggregate stage only a fifth of the peak value. On the other hand, the protein content of ECP increased drastically during the clump stage, and continued to slightly increase up to 11.4 μg/mg· biomass in the following last two stages. As a result, a remarkable change in the ratio of protein to carbohydrate of ECP was observed, as presented in Fig. 8-C. The ratio increased finally to 1/6 times as large as the initial value of 3.34.

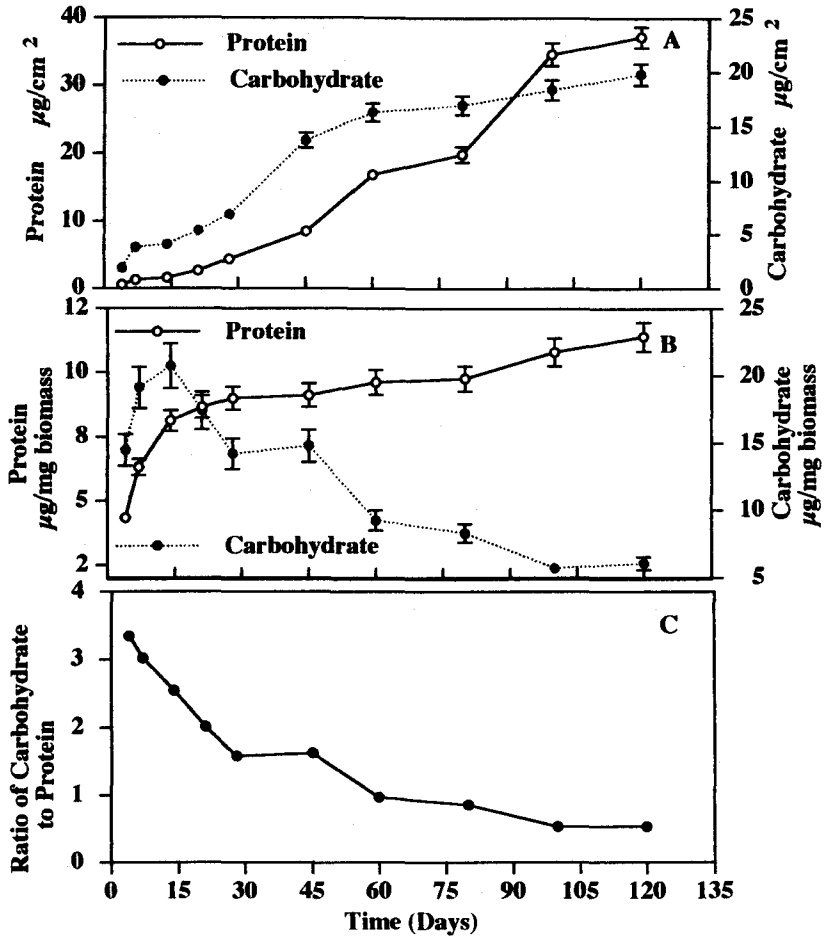

Fig.8 Behavior of extracellular polymer (ECP) during biofilm development. (Bars indicate SD, n=3)
A: Protein and carbohydrate contents of ECP as per substratum.
B: Protein and carbohydrate contents of ECP as per biomass.
C: The ratio of carbohydrate to protein of ECP.

Behavior of the viable cell number of methanogens (MPB) and propionate-degrading acetogen(PDA):

Fig. 9-A shows the results of MPN cell counting of biomass attached on glass-plates, with respect to acetoclastic methanogen (A-MPB) and hydrogeno- trophic methanogen (H-MPB) and pro- pionate-degrading acetogen (PDA). The viable cell number is expressed in cells per substratum area (MPN/cm^2) and in cell per dry cell weight (MPN/g biomass). The behavior of H-MPB was fairly different from that of A-MPB in the earlier stages. A sharp increment in H-MPB was observed in the adhesion stage, but in the following clump stage the number of H-MPB remained almost unchanged at 2.2×10^7 MPN/g· biomass (6.9×10^3 MPN/cm^2). H-MPB resumed to grow at the beginning of the conglomerate stage, and attained finally 1.6×10^9 MPN/g biomass (5.3×10^6 MPN/cm^2) in the aggregate stage.

The propagation of A-MPB in the earlier two (adhesion and clump) stages was not so fast as that of H-MPB was, but steadily lasted for 45—60 days. The final number of A-MPB at the end of the aggregate stage was of the same order of magnitude as H-MPB reached, i.e. 1.4×10^9 MPN/g· biomass.

The behavior of PDA was quite similar to that of A-MPB, exhibiting a steady increment during the clump stage. PDA attained ultimately 1.6×10^7 MPN/g· biomass (5.3×10^4 MPN/cm^2) in the aggregate stage, which was one to two orders of magnitude smaller than those of H-MPB and A-MPB.

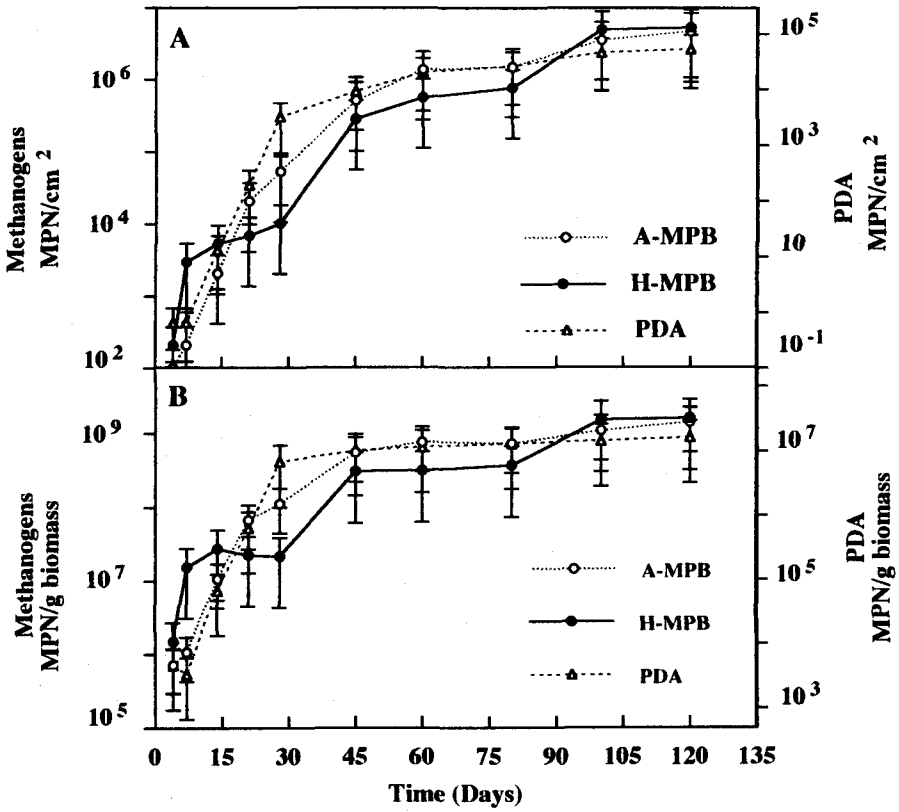

Fig. 9 The viable cell number of hydrogenotrophic, acetoclastic methanogen (H-MPB and A-MPB) and propionate-degrading acetogen (PDA). (Bars indicate 95% confidence limits)
A: MPN per substratum area. B: MPN per biomass.

Sulfate-reducing bacteria (SRB): Enumeration of SRB was also made using lactate, propionate and acetate as a respective electron donor, and the results were given in Fig.10. Fig.10 shows that there was a lag phase in proliferation of each trophic SRB. Among three trophic SRB, lactate-utilizing SRB (L-SRB) exhibited the highest level throughout the whole period, and attained 2.3×10^7 cfu/g· biomass (7.5×10^4 cfu/cm^2) at the final of the aggregate stage. The prevalence of propionate-utilizing SRB (P-SRB) was next to L-SRB, and the cell number of acetate-utilizing SRB (A-SRB) was smallest throughout. The number of P-SRB reached 1.0×10^6 cfu/g· biomass (3.4×10^3 cfu/cm^2) at the end of the aggregate stage. The final number of A-SRB was 3.0×10^5 cfu/g· biomass (1.0×10^3 cfu/cm^2) , which was two order of magnitude smaller than that of L-SRB. A significant increase in the cell number occurred in the clump stage for all the three trophic SRB.

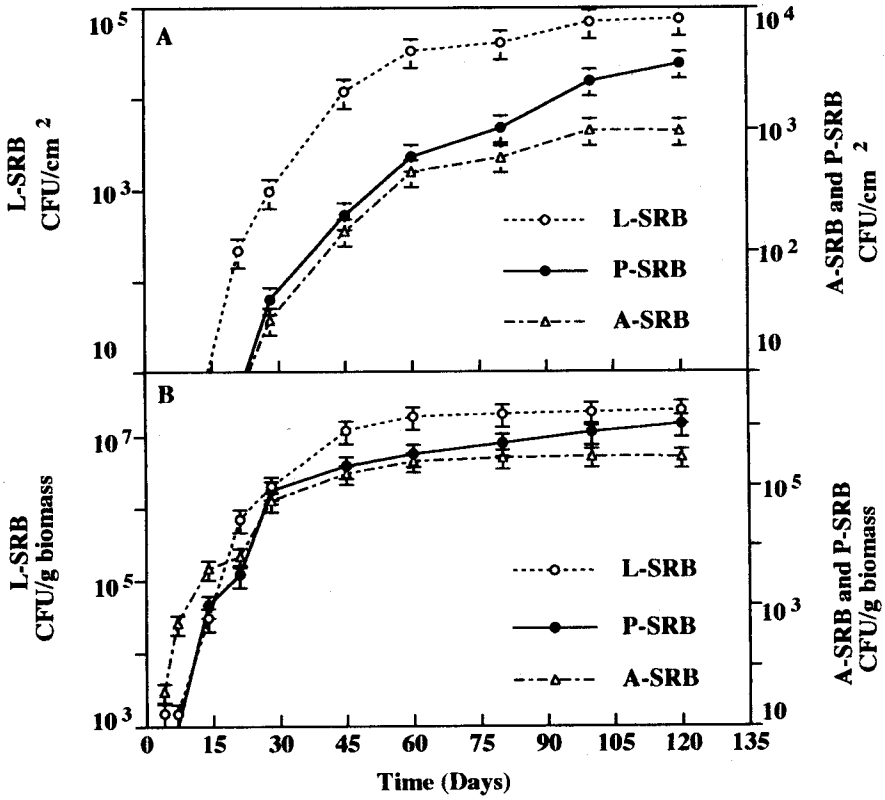

Fig. 10 The viable cell number of lactate-, acetate- and propionate consuming SRB. Bars indicate SD. (n=3) A: CFU per substratum area. B: CFU per biomass.

DISCUSSION

In the adhesion stage *Methanobrevibacter* spp. and *Methanothrix* spp. were able to promptly (within one day) attach to clean substrata whereas *Methanosarcina*-like organisms were not readily observed in this period. Since accumulation of ECP onto substratum surface was not substantial at that moment, the cell-surface hydrophobicity may be the most crucial factor to determine the initial adhesion. Grotenhuis *et. al.*[10] suggested that *Methanobrevibacter* spp. and *Methanothrix* spp. possess hydrophobic cell-surface properties. On the other hand, Verrier *et al.*[11]. reported that *Methanosarcina mazei* was much less able to adhere to any supports due to their high hydrophilic nature of cell surface. These both statements account well for our observation.

It was interesting that the carbohydrate content of ECP behaved in a different manner from the protein content. This denotes that the composition of ECP varied between each stage, affected by the shift in the predominant microflora. A remarkable increment in the carbohydrate content in the clump stage implies the polysaccharide component of ECP was more responsible for microbial attachment of organisms to directly substratum surface. Microscopic observation by Alcian-blue staining also supports the above-mentioned inference that initial adhesion was mediated by polysaccharide excretes. On the other hand, the increment of protein content during the later stages may be rather attributed to the accumulation cell-autolysis residuals.

A comparison of the structure of granular sludge with that of biofilm proved that there is a strong similarity in basic mechanisms of self-immobilization between biofilm formation and granulation. The most significant finding was that entangling structure of *Methanothrix* long-filaments played dual roles commonly in both processes. First, interwining web-network structure of *Methanothrix* filaments provided other bacterial groups with appropriate site for colonization (Figs.3-C and 6-C). MacLeod[12] also pointed out that the loose intertexture matrix of the filaments was suitable as microhabitats for other organisms. Secondly, stretch-out or elongated growth of the bacterium filaments is also favorable for formation of a further enlarged aggregate, by combing adjacent microcolonies with each other (Figs.2-C, 2-D and 6-D). Filamentous growth of the bacterium also seems to contribute for mechanical stability of biofilms and granules[13].

In the viable cell number counting, the methane contents in the MPN tubes of H-MPB were as high as 22—58% and those in A-MPB tubes were about 2—7% after 90 days incubation. The methane contents were always less than 0.8% in the control tubes . The *Methanothrix*-like organism was the dominant A-MPB in MPN tubes during the adhesion and the clump stages. After the clump stage, *Methanosarcina*-like organism became the predominant A-MPB in the highest dilution MPN counting tubes and the *Methanothrix*-like organism only appeared in lower dilution tubes. However, the reason that caused this phenomenon remains still unknown.

It is noteworthy that even though the retardation in attached-growth of A-MPB in the clump stage relative to that of H-MPB, the final population sizes of A-MPB and H-MPB were of the same order of magnitude. Much lower population size of PDA than that of MPBs (by a factor of two order of magnitude) may be partly accounted for by the fact that this bacterium requires strict symbiosis with hydrogen scavengers for existence. The other possible reason may be less capability of the bacterium in adhering to substratum, as pointed out by Yu and Pinder[14].

Comparison of the data given in Fig.9 and in Fig.10 indicates that SRB had more difficulty in adhesion than MPB. Among three trophic SRB, A-SRB exhibited the lowest significance of niche in the microbial ecosystem of biofilm. This tendency coincided with results of our previous study[15] that was obtained from granulated sludge grown in UASB reactors.

CONCLUSIONS

1. The overall process of anaerobic biofilm development could be differentiated into four stages according to the distinction in morphological changes: the adhesion, the clump, the conglomerate and the aggregate stages. Comparative microscopic observations of granular sludge suggested that there are a strong analogy in self-immobilization mechanisms between biofilm formation and granulation.
2. Filamentous growth of *Methanothrix*-like organism seemed to play important dual roles in biofilm formation and granulation processes. Web-network structures of entangling *Methanothrix*-filaments provided appropriate microhabitats for other trophic bacterial groups. Elongation of *Methanothrix*-filaments further served to conjoining adjacent microcolonies with each other to form extended aggregates.
3. The onset of the adhesion of hrdrogenotrophic methanogens occurred instantaneously within the first day. However, the final number of acetoclastic and hydrogenotrophic methanogen at the end of aggregate stage was the same order, i.e. $1.4—1.6 \times 10^9$/g· biomass. The cell number of propionate-degrading acetogen was two orders of magnitude smaller than those of methanogens.

REFERENCES

1. Harada H. (1988) Anaerobic Sludge Blanket Reactor (Capter 7) , in '*Wastewater Treatment by Immobilized-Microorganisms*", ed.by R. Sudo, Sangyo Yousui Chosakai, pp220-280 (in Japanese).
2. Lettinga G. and L.W. Hulshoff Pol (1991) UASB-process design for various types of wastewaters. Wat. Sci. Tech. 24: 87-107.
3. Harada H. (1988) Perspective on Research and Development on Treatment of Wastewaters by Microbial Self-immbilization Method, *Yosui-to-Haisui*, vol.31, No.1, pp5-11 (in Japanese)
4. Grotenhuis, J.T.C., J.C. Kissel, C.M. Plugge, A.J.M. Stams and A.J.B. Zehnder (1991) Role of substrate concentration in particle size distribution of methanogenic granular sludge in UASB reactors. Water Res. 25, 21-27.
5. Zeikus, J.G. (1977) The biology of methanogenic bacteria. Bacteria Rev. 41, 514-545.
6. Postgate, J.R. (1984) The sulfate reducing bacteria, 2nd ed., Cambridge University Press, London.
7. Morgan J.W., C.F. Forster, and L. Evison (1990) A comparative study of the nature of biopolymers extracted from anaerobic and activated sludges. Water Res. 24, 743-750.
8. Dubois M.J., Gilles K.A., Hamilton J.K., Reber P.A. and Smith F. (1956) Colometric method for determination of sugars and the related substances. Analy. Chem. 28, 350-356.
9. Lowry, O.H., N.J. Rosebrough, A.L. Farr, and R.J. Randall (1951) Protein J. Biol. Chem. 193. 265-275.
10. Grotenhuis, J.T.C., C.M. Plugge, A.J.M. Stams, and A.J.B. Zehnder (1992) Hydrophobicities and electrophoretic mobilities of anaerobic bacterial isolates from methanogenic granular sludge. Appl. Environ. Microbiol. 58: 1054-1056.
11. Verrier D., B. Mortier, H. C. Dubourguier and G. Albagnac. (1988) Adhesion of anaerobic bacteria to inert supports and development of methanogenic biofilms. In 5th international Symp. on Anaerobic Digestion. pp. 61-67.
12. MacLeod, F.A., Gioit, S.R. and Costerton, J.W. (1990) Layered structure of bacterial aggregates produced in an upflow anaerobic sludge bed and filter reactor. Appl. Environ. Microbiol. 56: 1298-1307.
13. Wiegant W.M. (1987) The 'spaghetti theory' on anaerobic sludge formation, or the inevitability of granulation. Proceeding of GASMAT-workshop. pp.146-152. Lunteren, Netherlands.
14. Yu, J.A. and K.L. Pinder (1992) Build-up of symbiotic methanogenic biofilms on solid support. Biotechnol. Letters. 14: 989-994.
15. Harada H., S. Uemura and K. Momonoi (1993) Interaction between sulfate-reducing bacteria and methane-producing bacteria in UASB reactors fed with low strength wastes containing different levels of sulfate. Water Res. 28,355-367.